Solid Freeform Fabrication 2017: Proceedings of the 28th Annual International Solid Freeform Fabrication Symposium – An Additive Manufacturing Conference
Reviewed Paper

Additive Manufacturing Utilizing Stock Ultraviolet Curable Silicone

Daniel A. Porter[1], Adam L. Cohen[1], Paul S. Krueger[1], and David Son[2]

[1] Dept. of Mechanical Engineering, Southern Methodist University Dallas, TX 75206
[2] Dept. of Chemistry, Southern Methodist University Dallas, TX 75206

Abstract

Extrude and Cure Additive Manufacturing (ECAM) is a method that enables 3D printing (3DP) of common thermoset materials. Ultraviolet (UV)-curable silicone is an example of a thermoset material with a large number of industrial and medical applications. 3D printed silicone prototype parts are obtained using a custom high pressure ram, valve, and UV exposure system.

This paper will address issues with printing stock UV curable silicone such as electrostatic repulsion, in-nozzle curing, and extrudate slumping. One solution that addresses two issues is adding carbon black (CB) to the mixture to reduce electrostatic repulsion while also inhibiting UV cure depth, hence preventing material from curing in the nozzle. Evidence shows that too much carbon black can be detrimental to the structural stiffness of the resulting part.

Introduction

Additive manufacturing (AM) is a lucrative and active research area with significant growth potential due to its myriad of commercial applications [1]. Common AM process materials such as acrylonitrile butadiene styrene (ABS), polylactic acid (PLA), polyamide (nylon), and photosensitive polymers are better understood, with more research attention focusing on the expansion of the viable AM material repertoire. 3D printing silicone is the leading edge of research in academic and industrial environments.

Polyurethanes, epoxies, urea formaldehyde, polyimides [2], and silicone rubber are thermoset materials that are difficult to 3D print via traditional additive manufacturing methods. Such techniques like material extrusion (ME) which include fused filament fabrication (FFF) are well researched for thermoplastics but are still being investigated for thermosets. Once crosslinking begins in the curing process for these materials, plastic reflow is impractical if not impossible. Introduced complexities may include unwanted cured material accumulation near the nozzle or part, system jams due to material curing in an improper place, mixing and system loading processes, and cleanup and maintenance after a print. Some benefits of using a ME setup for printing thermosets is the ability to utilize multiple materials (which is not compatible with stereolithography (SLA) and digital light processing (DLP)) not needing to encase the entire print bed to protect the curable material from initiators such as UV, and minimizing waste.

Although most materials that can be used in popular ME or FFF are of a rigid plastic nature, recently, advanced elastomers have been investigated in the field of additive manufacturing. Materials such as thermal plastic elastomers (TPE) [3] and silicones [4] [5] are now of interest. Silicone as a printing material for additive manufacturing is one of the newest additions to the 3D

printing field due to the numerous applications such as medical implants, component insulation, and prosthetics for their chemical, temperature, and moisture resistances along with mechanical flexibility, and weatherability [6] [7] [2].

San Draw Inc. (San Jose, CA) is able to print silicone in full color, adjustable hardness, and with multi-material capability [8]. San Draw Medical (San Jose, CA) is currently printing silicone seals for fuel cells [9]. Sterne Elastomere (Cavaillon, France) is revealing a silicone 3D printer that prints 0.25 mm layers of UV cured silicone [10]. Keyence, a Japanese sensor and printer manufacturer, is also developing a silicone 3D printing [11]. Stamos + braun Prothesenwerk (Dresden, Germany) is making headway into the biomedical field by 3D printing silicone inserts and bone structures [12]. Wacker Chemie (Munich Germany) announced the world's first industrial silicone 3D printer, the ACEO Imagine Series K [13], which utilizes drop on demand type printing for UV silicones. Fripp Design (Sheffield, U.K.) has the Picsima process which uses a needle to dispense a silicone component into a bath containing the other crosslinking component.

As of yet, UV curable silicones are not highly biocompatible, but the vast amount of non-medical silicone applications makes investigating additive manufacturing in this area still highly viable. Some polymer materials that are at least somewhat biocompatible include medical grade polyurethanes [14], polypyrrole [15], poly-ε-caprolactone [16], and silicones [17]. Other recent advances in additive manufacturing include printing optically transparent glass [18], polyvinylidene fluoride (PVDF) [19], and ultra-soft thermoplastic elastomers (TPE) [20]; fiber encapsulation additive manufacturing [21], printing of drug delivery devices [22], stretchable embedded sensors [23], and capacitive force sensors [24].

In this work Extrude and Cure Additive Manufacturing (ECAM) is performed at the Laboratory for Additive Manufacturing, Robotics, and Automation (LAMRA) to cure materials that are extruded and cured layer by layer or *in situ*. High pressures and friction inside the system create some difficulties for the given ME approach. Some of the greatest challenges are electrostatic repulsion, an effect that causes two masses to push apart due to significant charge of the same sign, and nozzle jamming. Carbon black is added to the UV curable silicone mix to reduce the repulsion effect and the amount of nozzle jams while curing *in situ*. The mechanical properties of 3D printed dog bones with different concentrations of carbon black are quantified and discussed in these proceedings.

Experimental Methods

Machine Setup

The custom ECAM machine built at LAMRA labs is shown Figure 1. A high-torque geared stepper motor drives a linear sled which in turn operates a high pressure hydraulic cylinder, Figure 1a). Material is loaded into the cylinder by pulling vacuum and in the case of high viscosity, assisted with a pressurized device. A manual valve at the end of the cylinder allows the material to be pushed through a Teflon high pressure hose, then high pressure metal tubing, and subsequently into a high pressure stainless steel pneumatically actuated valve shown in Figure 1b). From the pneumatic valve, material is deposited and positioned by the X and Y linear stages. The

constructed 3D printer with UV shielding is shown in Figure 1c). For silicones with additives, a filter is placed between the hydraulic cylinder and the metal plumbing on the Z stage.

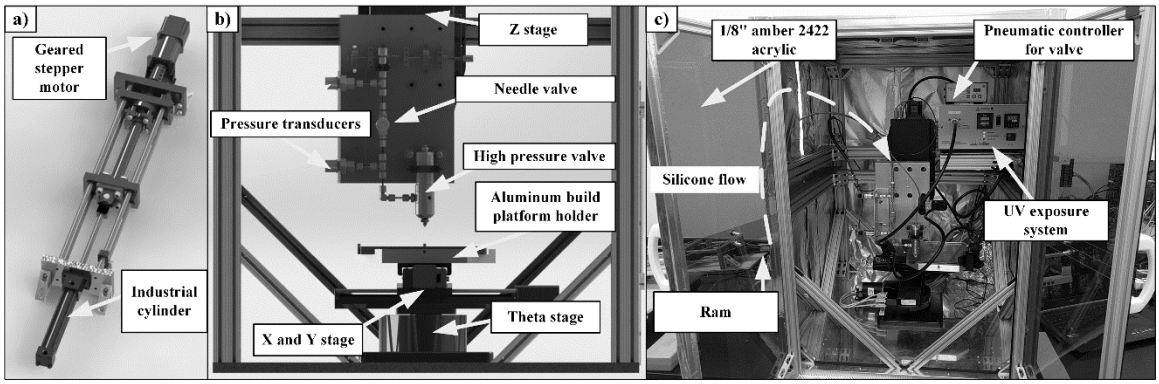

Figure 1. 3D printer utilized in this research. a) High pressure ram rendering, b) rendering of 3D printer, and c) constructed printer with valve controller and UV exposure system.

A custom UV wand holder is 3D printed in ABS and a render of the setup is shown in Figure 2. This custom holder ensured repeatability of prints by keeping the angle and distance of UV exposure wands fixed. The UV source is a Dymax Bluewave 200 (40 W/cm^2 total intensity) which has four wands optically coupled to the source. Four wands covered the immediate part being printed and ensured a cured layer for moderate part size despite extrusion direction. Brass nozzles with short throat lengths are used to ensure the pressure drop in the system is minimized.

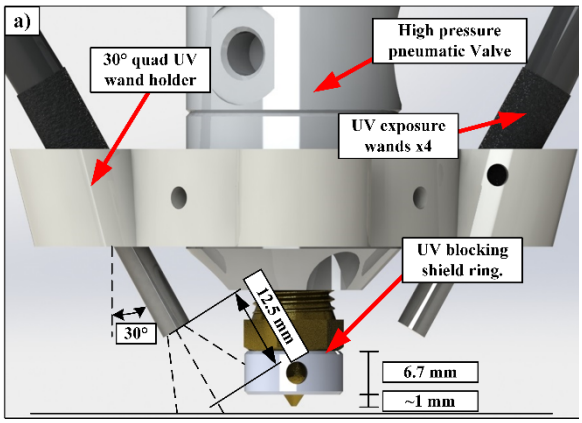

Figure 2. Custom UV wand holder and high pressure pnuematic valve setup with shield ring.

Initial Observations

Initial prints revealed problems such as significant slumping of certain materials, nozzle material accumulation (Figure 3b)), in nozzle curing (Figure 3a)), and electrostatic repulsion. Slumping was only a problem if the UV curable silicone was not cured immediately after extrusion. One way to get around the slumping problem was to print low aspect ratio beads. However this technique simultaneously increased cured material accumulation on the nozzle and interfered with the print process by rubbing against the part, reducing print quality and reliability. It became apparent that curing *in situ* was a preferred method when using low viscosity, non-shear-thinning materials. The material, if optically translucent, may act as a light guide and gradually cure material in the nozzle thus clogging the system.

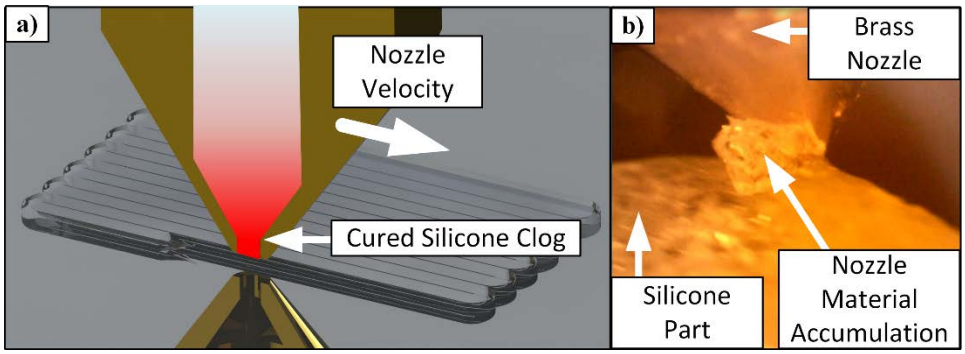

Figure 3. a) Rendering of a typical silicone nozzle clog in which the material cures in the dispense orifice and b) an image of nozzle material accumulation.

Electrostatic repulsion is observed in this system configuration with silicones from Momentive Performance Materials (Waterford, NY). The effect seems greater in higher viscosity materials like UV Silopren 2030 when compared to UV Electro 225-1 which has viscosities of ~450 Pa-s and ~70 Pa-s respectively at 10 s^{-1} according to Momentive's technical data sheet. After a few minutes of material extrusion, the silicone upstream of the nozzle starts to locally accumulate electrostatic charge. Combined with the charging that occurs during UV curing, the resulting effect is a significant repulsion force acting on the extruded silicone. This can be observed by the extrudate deviating from its intended deposition path, degrading part geometry and potentially mechanical quality to suffer. Illustrating this effect is Figure 4d) and f). The silicone used in Figure 4 is UV Silopren 2030 and is shown as a free stream in Figure 4a). Observe the lack of an electrostatic repulsion effect to a black nitrile glove in Figure 4b), an uncured blob of silicone in Figure 4c), and an aged 3D printed silicone part in Figure 4e). Contrast this to a freshly 3D printed silicone part in Figure 4d) and cured silicone blob in Figure 4f). Diversion of the viscous fluid indicates electrostatic repulsion effects.

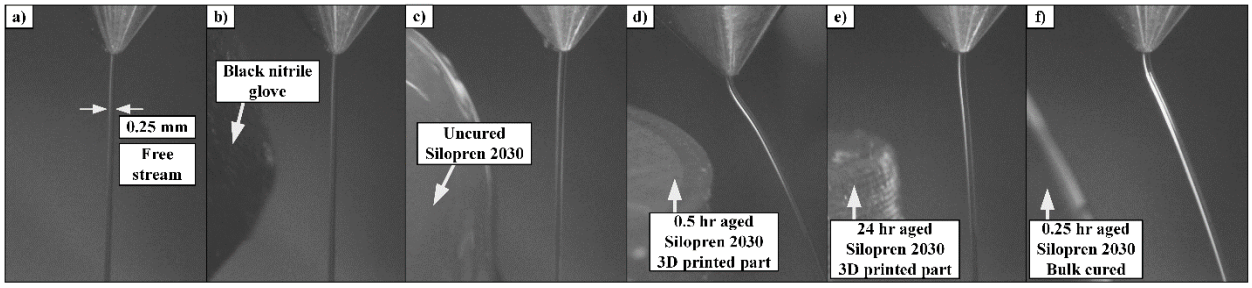

Figure 4. Repulsion effects for a) free stream of UV Silopren 2030 next to b) a nitrile glove, c) an uncured blob of silicone, d) a recent 3D printed silicone part, e) an aged 3D printed silicone part, and f) a bulk UV cured blob of silicone.

Reducing the repulsion effect would require eliminating or neutralizing the surface charge of the part, the tribocharged silicone emerging from the nozzle, or both. Adding electrically conductive fillers can ameliorate this problem. Options for electrically conductive fillers include antimony-tin doped oxide [25], aluminum, silver, copper, silicon-carbide [26], ZnO [27], carbon black (CB) powder [28], carbon nanotubes [29], among others. The carbon black option is inexpensive and simple but also increases the opaqueness of the silicone, thus impeding the curing

depth. Impeding the curing depth can be detrimental to part mechanical properties but could also alleviate some problematic observation like silicone curing in the nozzle.

CB in silicone has been explored before with research being done to understand the benefits and effects [30] [28] [31] [32]. Electrical conductivity percolation thresholds for carbon black in a medium vary significantly, but some typical values are 10-25 percent by volume when in a styrene butadiene rubber (SBR) [33]. The objective is to not make the silicone as conductive as a bulk material, but rather to reduce the localized tribocharging which appears to cause the electrostatic repulsion. With this in mind, UV Electro 225-1 is mixed with small amounts of Vulcan XC605 carbon black from Cabot (Boston, MA). All samples tested and printed were mixed with a FlackTek Speedmixer^{TM} DAC 150.1 FVZ-K (Landrum, SC) to ensure thorough dispersion of the CB. The samples were mixed at 2500 RPM for 150 seconds, then the composite was scraped off the inner sides of the container and mixed again. Even with the Speedmixer, there are conglomerates of CB that exist which clog the nozzle and require in line system filtering.

Quantifying Slumping of Silicone

Understanding how much a material slumps is important to 3D printing. It is vital to know just how the height of a bead changes as a function of time. To obtain this information ten traces of UV Electro 225-1 and UV Silopren are printed 100 mm long at 20 mm/s. A dwell time of about 30 seconds is held in-between each trace giving a total dwell time range of about 300 seconds. Immediately after the ten traces are printed a UV flood exposure is done at max intensity so that all of the silicone lines are cured as fast as possible. Traces of 0.25, 0.20, and 0.10 mm height are printed and have an equivalent flow rate that would allow for a 0.5 mm wide trace assuming a pill shaped cross section.

The glass substrate with the printed silicone lines is taken to a microscope, Olympus (Shinjuku, Tokyo, Japan) BX60, where a marking compound is drawn across a section of each trace to improve measurability. Height measurements are performed by focusing on the glass substrate and then on top of the marked trace while a Fowler (Newton, MA) Digital Indicator to measure the displacement. Extrudate widths are measured using a digital microscope camera from Dino Lite (New Taipei City, Taiwan) AM-7023B. These experiments are repeated three times for each type of silicone and trace height and then averaged. Figure 5 shows the glass plate with three sets of slumping experiments right after UV exposure.

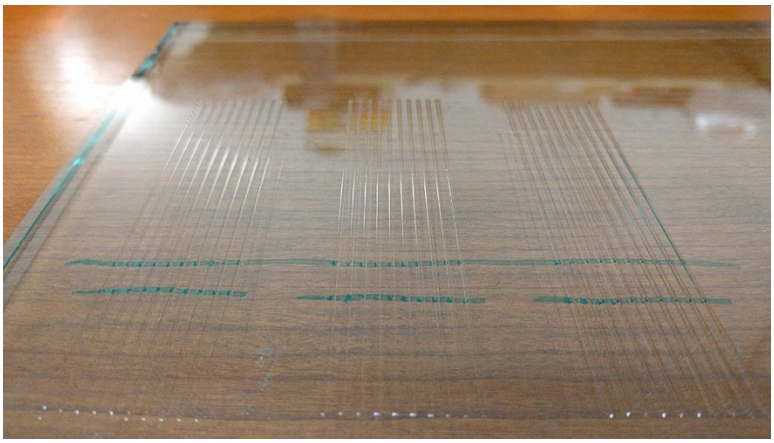

Figure 5. Three sets of cured UV Electro 225-1 traces with a light marking compound applied.

Mechanical Property Testing

Dog bone structures adhering to ASTM standard D638 T1 are 3D printed in UV Electro 225-1 with different loadings of CB. For comparison, bulk cast molds of the same dog bone are done for the same material. Print specifications for the samples are shown in Table 1. There are five prepared samples for each dog bone lot.

Table 1. Printing parameters for dog bone samples.

Parameter	Value	Notes
Feed rate (mm/s)	15	X, Y total vector velocity
Layer height (mm)	0.25	
Extrudate width (mm)	0.50	Trace to trace spacing
Infill %	100	
Infill pattern type	Rectilinear	Alternates by 90 degrees each layer
Infill angle (deg)	45	
Outer perimeters	3	
UV wand distance (mm)	~15	From wand to plane surface
UV wand angle (deg)	30	Measured from vertical

The samples are covered in talc powder and marked so that the gauge length marks (50mm) may easily be observed with a HD camera. Each sample is loaded into a tensile testing apparatus and strained at 500 mm/min until an end displacement of 100 mm is achieved. Pictures are captured intermittently from above while force data is recorded. The tensile testing apparatus with a bulk 0.00 and 3D printed 0.15wt% loaded is shown in Figure 6a) and Figure 6b). A single sample from the bulk and 0.00, 0.15, 0.50, and 1.00 wt% CB 3D printed dog bones is shown in Figure 6c) through g).

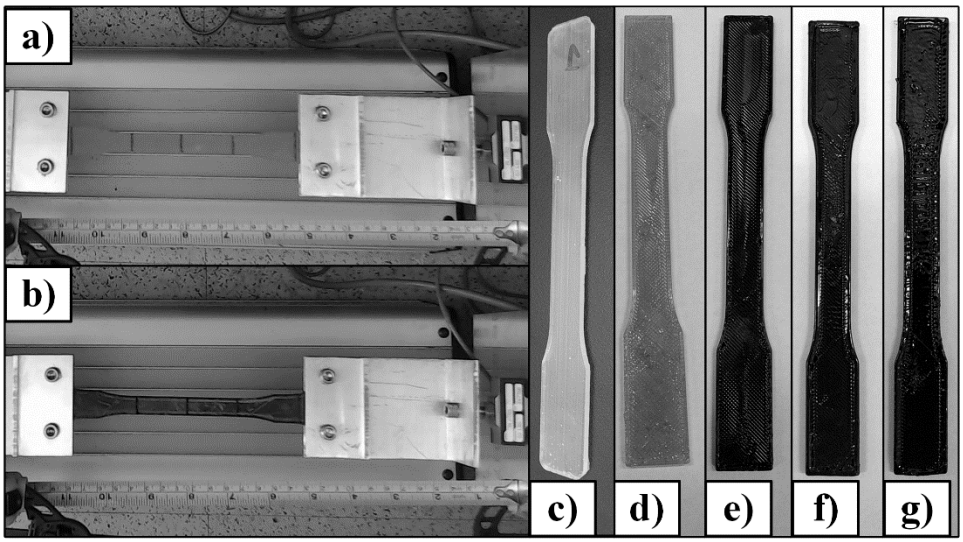

Figure 6. Dog bones with 0.00 wt% and 0.15 wt% CB marked and loaded into the tensile tester. Bulk dog bone with c) 0.00 wt% and 3D printed UV Electro 225-1 dog bones with d) 0.00, e) 0.15, f) 0.50, and g) 1.00 wt% CB loading.

Hardness of all samples is measured using a Rex DD-4 Type M durometer (Rex Durometers, Buffalo Grove, IL) and with LabVIEW (National Instruments, Austin, TX) data logging software. Measurements are taken on three different positions on the samples and then averaged. Hardness is a good indicator of how well cured each sample is.

Results and Discussion

Carbon Black Effect on Repulsion

Different amounts of CB are added to Silopren 2030 and bulk cured under a UV wand for around 3 minutes. The larger the wt% of CB, the thinner the layer of cured silicone in the bulk solid due to the CB attenuating the curing depth of the UV. Repulsion effects for the different wt% loadings in UV Silopren 2030 are shown in Figure 7a) through e). Figure 7f) shows that a freshly printed part in UV Electro 225-1 next to a stream of the same material having the same CB loading has negligible repulsion effects.

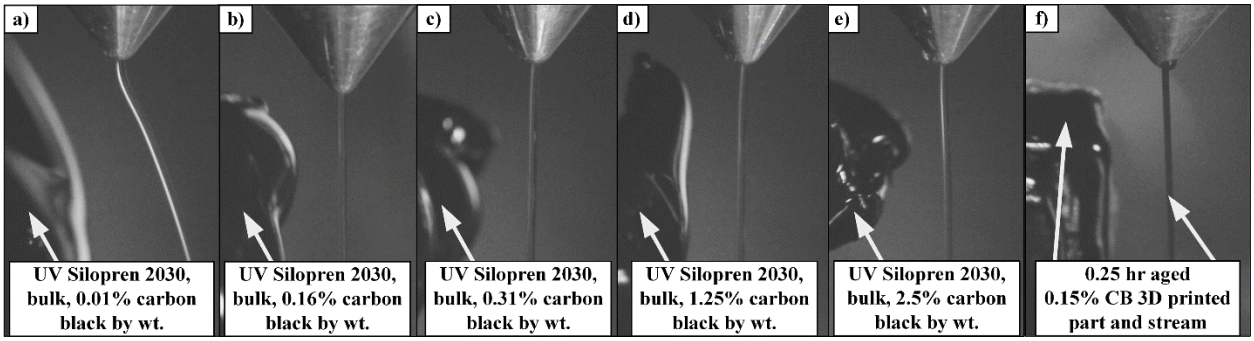

Figure 7. Effects of a) 0.01 wt%, b) 0.16 wt%, c) 0.31 wt%, d) 1.25 wt%, and e) 2.50 wt% bulk cured CB loaded UV Silopren 2030 on the repulsion effect given a 0.00 wt% CB free stream of the same material. A 0.15 wt% CB free stream of UV Electro 225-1 f) flows next to a freshly 3D printed silicon part fabricated with the same silicone.

In addition to the reduction of the electrostatic repulsion, all prints with carbon black loading of 0.15 wt% or higher showed a significant decrease in the occurrence of nozzle jams that were caused by silicone curing in the dispense orifice. In fact there was only one jam which occurred when 3D printer was left idle for about 30 minutes while the UV exposure system was active. Nozzle material accumulation was lessened with the same amount of carbon black but eventually still occurs with the given setup.

Slumping of Silicone

Results for slumping of UV Electro 225-1 and UV Silopren 2030 are shown in Figure 8. From Figure 8a) and b). The slopes of width versus dwell time are greater for the less viscus silicone UV Electro 225-1. Also the heights in Figure 8c) and d) show the same general trend that UV Electro drops faster than UV Silopren 2030. Images of UV Electro 225-1 after 30 seconds of dwell time, Figure 9 a), show widening by 20 percent. 300 seconds of dwell time for UV Silopren 2030 start to show significant widening, Figure 9 b).

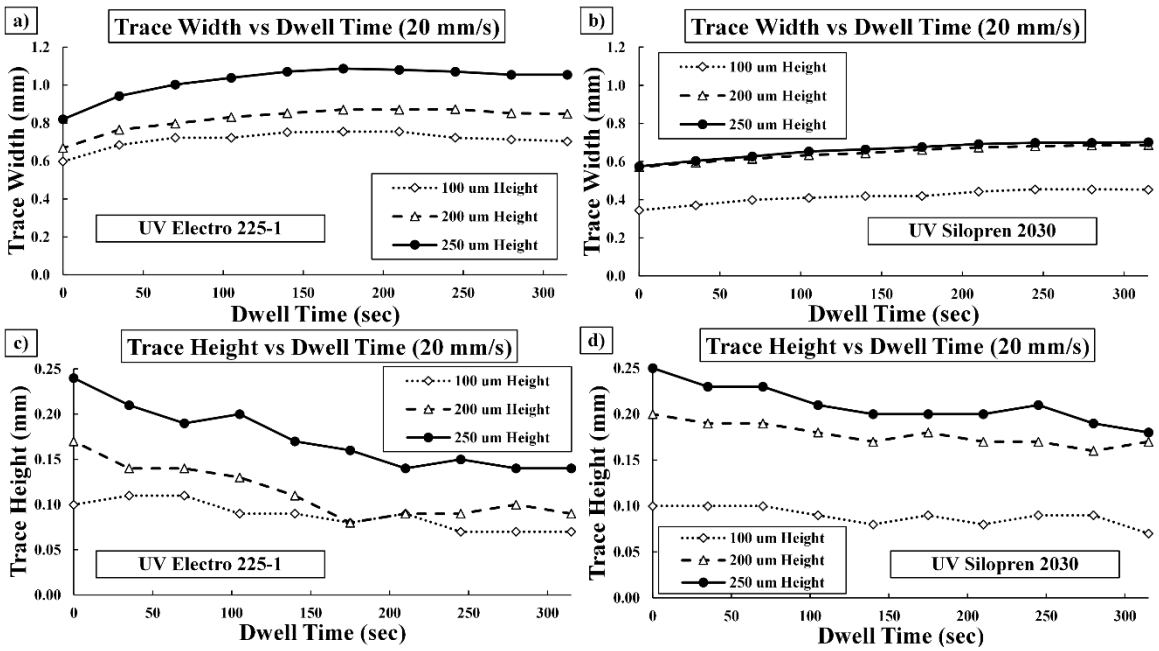

Figure 8. Slumping result widths for a) UV Electro 225-1 and b) UV Silopren 2030. Slumping result heights for c) UV Electro 225-1 and d) UV Silopren 2030.

The results of the slumping test show the importance of needing to cure *in situ* for materials like UV Electro 225-1. These experiments were performed on glass substrates so the results of slumping may be slightly different for a substrate of tacky silicone of the same type. This would reveal the effect of wettability on slumping.

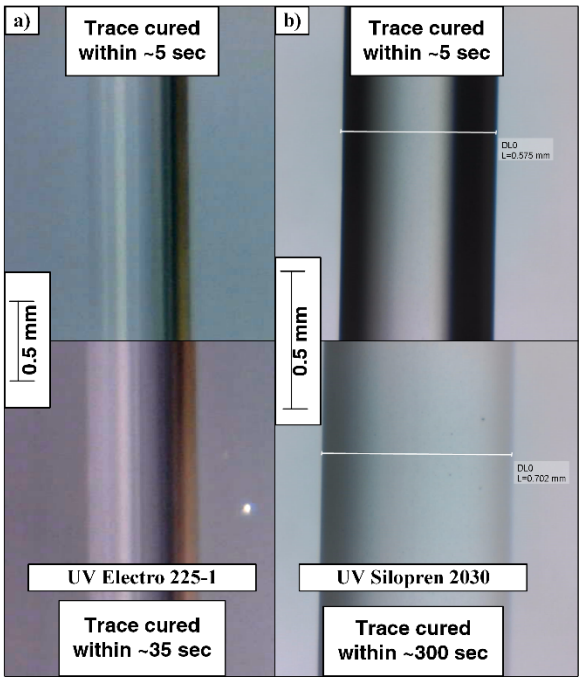

Figure 9. Images of a) UV Electro 225-1 trace after 30 seconds of dwell time b) vs UV Silopren 2030 after 300 seconds.

Stiffness of Dog Bone Samples

Initial dog bone tensile testing revealed that the bulk, 0.00, and 0.15 wt% CB dog bone samples have almost equivalent stiffness responses. The stiffness results are averaged for all five samples in each category for simplicity. The higher 0.50 and 1.00 wt% CB samples had much lower stiffness values as shown in Figure 10a). Secant modulus results for the stress versus strain curves are shown in Figure 10b). A drop in stiffness for higher loaded CB dog bones was expected because UV curing starts to become significantly attenuated enough that the bottom part of the 3D printed traces are not fully cured by the time the entire layer is finished.

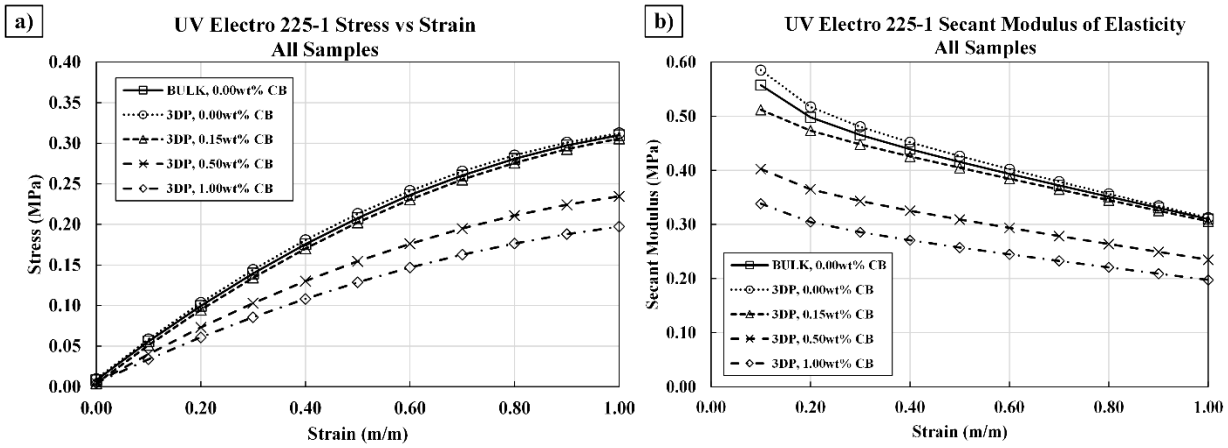

Figure 10. Tensile test results for all as cast and as printed dog bone samples.

UV Electro 225-1 was found to be fully cured after baking in an oven at 121°C for 10 minutes. Three of the dog bone samples were put into an oven and baked for the same settings to see if stiffness and hardness improvments could be made. The average stiffness response for the three dog bones in the post-oven cured experiment are shown in Figure 11. It is evident from Figure 11 that post-oven curing the bulk and 3D printed samples will fully cure the silicone. An enhancement in stiffness over simple UV curing is also observed with post-oven processing at the prescribed time and temperature.

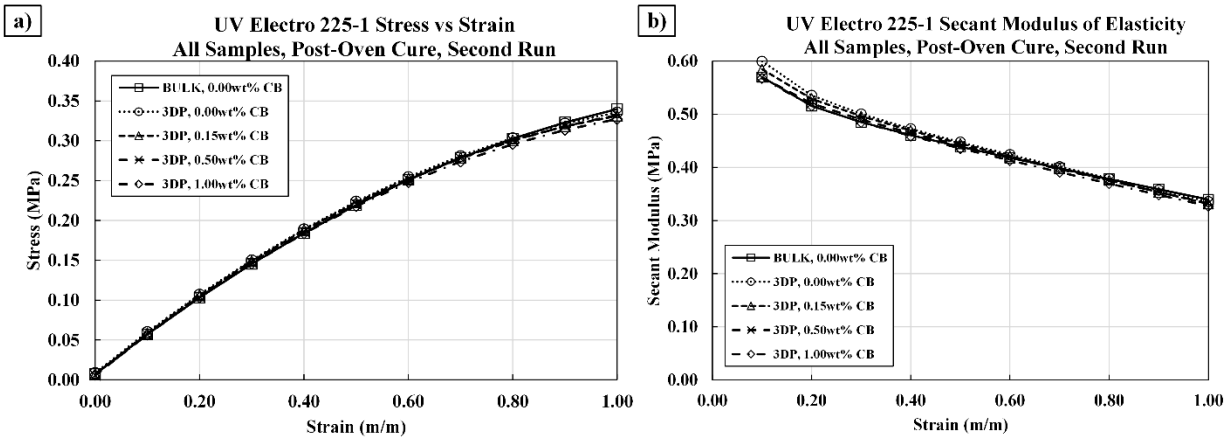

Figure 11. Post-oven cure tensile test results for cast and printed dog bone samples.

Quantifications for dog bone tensile testing is shown in Table 2 along with the standard deviation for 100% strain measurements. For UV Electro 225-1, a CB wt% of 0.15 gave the best benefit in terms of alleviating nozzle clogging and electro static repulsion while still maintaining a comparable stiffness to the bulk and 0.00wt% CB 3D printed samples.

Table 2. Tensile test results for all dog bone samples showing modulus at 100% strain. Percent difference is with reference to the initial tensile testing results.

	Modulus 100% (MPa), initial		Modulus 100% (MPa), post-oven cure		
	Average	Std. Dev.	Average	Std. Dev.	% Diff
Bulk Cast	0.310	0.004	0.340	0.008	9.59
3D Printed, 0.00 wt% CB	0.312	0.007	0.336	0.004	7.45
3D Printed, 0.15 wt% CB	0.306	0.008	0.331	0.007	8.36
3D Printed, 0.50 wt% CB	0.235	0.017	0.332	0.008	41.61
3D Printed, 1.00 wt% CB	0.197	0.007	0.327	0.007	65.82

Hardness of Dog Bone Samples

Durometer results for the dog bone samples also reveal that 0.50 and 1.00 wt% CB samples are under cured compared to the others. Once post-oven cured, the samples increased in Durometer like the results of the stiffness tests. Momentive reports that the durometer for a fully cured UV Electro 225-1 sample is about Shore 25 A which correlates to about ~26-27 Shore M (assuming sample thickness is not small) indicating the bulk cast, 3D printed 0.00, and 0.15 wt% carbon black samples are most likely fully cured via UV exposure.

Table 3. Durometer results for all dog bone samples. Percent difference is with respect to initial durometer measurements.

	Hardness, M initial		Hardness, M post-oven cured		
	Average	Std. Dev.	Average	Std. Dev.	% Diff
Bulk Cast	26.8	1.05	26.7	0.59	-0.48
3D Printed, 0.00 wt% CB	26.1	1.30	26.0	0.20	-0.29
3D Printed, 0.15 wt% CB	26.1	0.31	26.5	0.17	1.55
3D Printed, 0.50 wt% CB	24.6	1.03	26.9	0.54	9.25
3D Printed, 1.00 wt% CB	22.6	1.03	27.4	0.27	21.26

Conclusions and Future Work

UV curable silicone dog bone samples are 3D printed with a high pressure ECAM system. Slumping of silicones is investigated and is found to be significant for the low viscosity and non-shear-thinning UV Electro 225-1 thus leading to the need of *in situ* curing. Problems with *in situ* curing using stock silicone materials are in nozzle curing, nozzle material accumulation, and electrostatic repulsion. Carbon black is selected as an inexpensive additive and was found to

significantly stop system jams due to silicone curing in the nozzle and reduce the amount of nozzle material accumulation.

Material property tests revealed that bulk cast, 0.00 and 0.15 wt% CB 3DP dog bones responded approximately the same to applied force. The 0.50 and 1.00 wt% CB loaded 3DP dog bones showed lower stiffnesses indicating that they were not fully UV cured. This could be detrimental to printing silicone parts that have high aspect ratios as the entire part could accumulate a large Z height error due to weight. A post-oven cure on three of the samples from each lot increased all of the dog bone stiffnesses to levels comparable to bulk cured material. Thus a small amount of carbon black in UV silicones can allow for continuous high intensity *in situ* UV curing to minimize slumping effects while retaining mechanical stiffness and harnesses. One downside is that the color of the silicone is tinted.

Work to eliminate nozzle material accumulation currently entails using UV opaque materials with smooth surfaces and nonstick properties. The printing process must be optimized because silicone may still cure around the nozzle in a ring shape which could mechanically lock itself in place. Inexpensive additives that reduce slumping and inhibit UV curing depth while retaining translucent optical properties are also being investigated.

References

[1] Stansbury JW, Idacavage MJ. 3D printing with polymers: Challenges among expanding options and opportunities. DENT MATER. 2016;32(1):54–64.

[2] Plastics M, Harper CA. Modern Plastics Handbook. Harper CA, editor. McGraw-Hill; 1999.

[3] Saari M, Cox B, Galla M, Krueger PS, Richer E, Cohen AL. Multi-material additive manufacturing of robot components with integrated sensor arrays. In: Proc. of SPIE. vol. 9494; 2015.

[4] Duoss EB, Weisgraber TH, Hearon K, Zhu C, Small W, Metz TR, et al. Three-dimensional printing of elastomeric, cellular architectures with negative stiffness. ADV FUNCT MATER. 2014;24(31):4905–4913.

[5] Jin Y, Plott J, Shih AJ. Extrusion-based Additive Manufacturing of the Moisture-Cured Silicone Elastomer. In: SOL FREEFORM FABRIC; 2015.

[6] NIIR Board of Consultants & Engineers. The Complete Technology Book on Industrial Polymers. Additives. Colourants and Fillers. Asia Pacific ND, editor. National Institute of Industrial Research; 2006. ISBN: 8178330091.

[7] NIIR Board of Consultants & Engineers. The Complete Book on Rubber Processing and Compounding Technology (with Machinery Details). 2nd ed. Inc APBP, editor. National Institute of Industrial Research; 2010. ISBN: 8178330059.

[8] Tess at 3Ders.org. San Draw's innovative FAM Technology offers full-color silicone 3D printing with adjustable hardness. http://www.3ders.org/articles/20160617-san-draws-fam-3d-printer-makes-multi-color-silicone-models-for-medical-industry.html; 2016. Last accessed May 2nd, 2017.

[9] Scott C at 3Dprint.com. 3D Printed Silicone Seals for Fuel Cells Lead to New Service from San Draw. https://3dprint.com/149248/san-draw-3d-printed-seals/; 2016. Last accessed May 2nd 2017.
[10] Scott C at 3Dprint.com. Sterne Elastomere Unveils SiO-Shaping 1601 Silicone 3D Printer at K 2016. https://3dprint.com/153427/sterne-elastomere-silicone-printer/; 2016. Last accessed May 2nd, 2017.
[11] Buren A at 3Ders.org. 3D printer manufacturer Keyence introduces silicone based 3D printing material. http://www.3ders.org/articles/20161011-3d-printer-manufacturer-keyence-introduces-silicone-based-3d-printing-material.html; 2016. Last accessed May 2nd, 2017.
[12] Prothesenwerk.com. 3D-printing of Biomedical Grade Silicones. http://www.prothesenwerk.com/en/f156000172.html;. Last accessed May 2nd 2017.
[13] Grunwald S at 3Dprint.com. Wacker Chemie Will Debut the First Industrial 3D Printer for Silicones at K 2016. https://3dprint.com/141718/wacker-3d-printer-silicones/; 2016. Last accessed November 21st, 2016.
[14] Chen H, Yuan L, Song W, Wu Z, Li D. Biocompatible polymer materials: Role of protein-surface interactions. PROG POLYM SCI. 2008;33(11):1059–1087.
[15] George PM, Lyckman AW, LaVan DA, Hegde A, Leung Y, Avasare R, et al. Fabrication and biocompatibility of polypyrrole implants suitable for neural prosthetics. BIOMATERIALS. 2005;26(17):3511–3519.
[16] Sinha VR, Bansal K, Kaushik R, Kumria R, Trehan A. Poly-epsilon-caprolactone microspheres and nanospheres: an overview. INT J PHARM. 2004;278(1):1–23.
[17] Shastri VP. Non-degradable biocompatible polymer in medicine: past, present and future. CURR PHARM BIOTECHNO. 2003 October;4(5):331–337.
[18] Klein J, Stern M, Franchin G, Kayser M, Inamura C, Dave S, et al. Additive manufacturing of optically transparent glass. 3D PRINT ADDIT MANUF. 2015;2(3):92–105.
[19] Porter DA, Hoang TVT, Berfield TA. Effects of in-situ poling and process parameters on fused filament fabrication printed PVDF sheet mechanical and electrical properties. ADDIT MANUF. 2017 January;13:81–92.
[20] Saari M, Xia B, Krueger PS, et al. Additive Manufacturing of Soft Parts from Thermoplastic Elastomers. In: 12th TPE Topical Conference; 2016. .
[21] Saari M, Bryan C, Edmond R, Krueger P, Cohen A. Fiber Encapsulation Additive Manufacturing: An Enabling Technology for 3D Printing of Electromechanical Devices and Robotic Components. 3D PRINT ADDIT MANUF. 2015 March;2(1):32–39.
[22] Norman J, Madurawe RD, Moore CMV, Khan MA, Khairuzzaman A. A New Chapter in Pharmaceutical Manufacturing: 3D-Printed Drug Products. ADV DRUG DELIVER REV. 2016 January;108(1):39–50.
[23] Muth JT, Vogt DM, Truby RL, Mengüç Y, Kolesky DB, Wood RJ, et al. Embedded 3D printing of strain sensors within highly stretchable elastomers. ADV MATER. 2014;26(36):6307–6312.
[24] Saari M, Xia B, Cox B, Krueger PS, Cohen AL, Richer E. Fabrication and Analysis of a Composite 3D Printed Capacitive Force Sensor. 3D PRINT ADDIT MANUF. 2016;3(3):136–141.
[25] Wei HJ, Cherney EA, Jayayam S. Improvements to the Performance of Silicone Rubber Housed Composite Bushings by means of a Resistive Coating. In: IEEE INT SYM ELEC IN; 2004. p. 324–327.

[26] Quereshi AH, Raghuveer MR. Partially Conducting Insulation Materials for High Voltage Overhead Applications. In: Proceedings of the 14th Electrical/Electronics Insulation Conference; 1979. p. 272–274.
[27] Vaughan A. Polymer Surfaces: Designing Materials to Prevent or Withstand Discharge Activity. In: IEE Colloquium on Surface Phenomena Affecting Insulator Performance; 1998. p. 9/1–9/3.
[28] Luheng W, Tianhuai D, Peng W. Effects of conductive phase content on critical pressure of carbon black filled silicone rubber composite. SENSORS ACTUAT A-PHYS. 2007;135(2):587–592.
[29] Liu C, Fan S. Nonlinear electrical conducting behavior of carbon nanotube networks in silicone elastomer. APPL PHYS LETT. 2007;90(4):041905.
[30] Luheng W, Tianhuai D, Peng W. Influence of carbon black concentration on piezoresistivity for carbon-black-filled silicone rubber composite. CARBON. 2009;47(14):3151–3157.
[31] Wang L, Ma F, Shi Q, Liu H, Wang X. Study on compressive resistance creep and recovery of flexible pressure sensitive material based on carbon black filled silicone rubber composite. SENSORS ACTUAT A-PHYS. 2011;165(2):207–215.
[32] Kost J, Foux A, Narkis M. Quantitative model relating electrical resistance, strain, and time for carbon black loaded silicone rubber. POLYM ENG SCI. 1994 November;34(21):1628–1634.
[33] Karasek L, Meissner B, Asai S, Sumita M. Percolation Concept: Polymer-Filler Gel Formation, Electrical Conductivity and Dynamic Electrical Properties of Carbon-Black-Filled Rubbers. POLYM J. 1996;28(2):121–126.